J|A|C|S
ARTICLES
Published on Web 03/10/2007

Cation−Anion Interactions as Structure Directing Factors: Structure and Bonding of Ca_2CdSb_2 and Yb_2CdSb_2

Sheng-qing Xia and Svilen Bobev*

Contribution from the Department of Chemistry and Biochemistry, University of Delaware, Newark, Delaware 19716

Received December 23, 2006; E-mail: bobev@udel.edu

Abstract: Two new transition-metal-containing Zintl phases, Ca_2CdSb_2 and Yb_2CdSb_2, have been synthesized by flux reactions, and their structures have been determined by single-crystal X-ray diffraction. Yb_2CdSb_2 crystallizes in the noncentrosymmetric orthorhombic space group $Cmc2_1$ (No. 36, $Z = 4$). Ca_2CdSb_2 crystallizes in the centrosymmetric orthorhombic space group *Pnma* (No. 62, $Z = 4$). Despite the similarity in their chemical formulas and unit cell parameters, the structures of Yb_2CdSb_2 and Ca_2CdSb_2 are subtly different: Ca_2CdSb_2 has a layered structure built up of infinite layers of $CdSb_4$ tetrahedra connected through corner-sharing. These layers are stacked in an alternating $\mathbf{AA^{-1}AA^{-1}}$ sequence along the direction of the longest crystallographic axis (**A** denotes a layer; $\mathbf{A^{-1}}$ stands for its inversion symmetry equivalent), with Ca^{2+} cations filling the space between them. The structure of Yb_2CdSb_2 features the very same $[CdSb_2]^{4-}$ layers of $CdSb_4$ tetrahedra, which because of the lack of inversion symmetry are stacked in an **AAAA**-type fashion and are separated by Yb^{2+} cations. Electronic band structure calculations performed using the TB-LMTO-ASA method show a small band gap at the Fermi level for Ca_2CdSb_2, whereas the gap closes for Yb_2CdSb_2. These results suggest narrow gap semiconducting and poorly metallic behavior, respectively, and are confirmed by resistivity and magnetic susceptibility measurements. The structural relationship between these new layered structure types and some well-known structures with three-dimensional four-connected nets are discussed as well.

1. Introduction

Zintl phases are intermetallic compounds that are made up of metals with very different electronegativities, most commonly the alkali and alkaline-earth metals and the early to late post-transition metals and semimetals.[1−3] In the past 15−20 years, extensive research efforts in the area have led to the extension of this classification to include some lanthanide elements, as well as a variety of transition metals.[4−7] Hence, the crystal chemistry of these compounds brings together the most unique combination of metal−metal interactions that are not characteristic for the typical covalent or the typical ionic solids. As a result, Zintl phases have diverse and complicated structures and quite often exhibit a variety of unprecedented physical properties.[1−7]

The inherent complexity of the crystal and electronic structures transpires into serious difficulties in rationalizing the structure−property relationships in such compounds. The classic Zintl reasoning, which assumes a complete valence electron transfer from the less electronegative elements to the more electronegative ones so that each element achieves a closed-shell state conforming to the octet rule, works satisfactory only for a limited number of cases. More frequently, the interactions in nonclassic Zintl phases (majority cases) are intermediate between the localized 2-center-2-electron and the delocalized multicenter bonding, i.e., full electron transfers and realization of noble-gas configurations are rarely achieved. This holds particularly true for structures containing elements with not very different electronegativities, where structure descriptions in terms of covalently bound polyanionic subnetwork and spectator cations (providing simply the necessary bonding electrons and

(1) (a) Schäfer, H; Eisenmann, B.; Müller, W. *Angew. Chem., Int. Ed. Engl.* **1973**, *12*, 694−712. (b) Corbett, J. D. *Angew. Chem., Int. Ed.* **2000**, *39*, 670−690.
(2) (a) Kauzlarich, S. M., Ed. *Chemistry, Structure and Bonding in Zintl Phases and Ions*; VCH: New York, 1996, and the references therein. (b) Miller, G. J. *Eur. J. Inorg. Chem.* **1998**, 523−536.
(3) Nesper, R. *Angew. Chem., Int. Ed. Engl.* **1991**, *30*, 789−817.
(4) (a) Gascoin, F.; Sevov, S. C. *Angew. Chem., Int. Ed.* **2002**, *41*, 1232−1234. (b) Gascoin, F.; Sevov, S. C. *Inorg. Chem.* **2002**, *41*, 2820−2825. (c) Gascoin, F.; Sevov, S. C. *Inorg. Chem.* **2002**, 41, 5920−5924. (d) Gascoin, F.; Sevov, S. C. *Inorg. Chem.* **2003**, *42*, 904−907.
(5) (a) Kuromoto, T. Y.; Kauzlarich, S. M.; Webb, D. J. *Chem. Mater.* **1992**, *4*, 435−440. (b) Kim, H.; Condron, C. L.; Holm, A. P.; Kauzlarich, S. M. *J. Am. Chem. Soc.* **2000**, *122*, 10720−10721. (c) Holm, A. P.; Park, S. M.; Condron, C. L.; Kim, H.; Klavins, P.; Grandjean, F.; Hermann, R. P.; Long G. J.; Kanatzidis, M. G.; Kauzlarich, S. M.; Kim, S. J., *Inorg. Chem.* **2003**, *42*, 4660−4667. (d) Holm, A. P.; Olmstead, M. M.; Kauzlarich, S. M. *Inorg. Chem.* **2003**, *42*, 1973−1981. (e) Jiang, J.; Payne, A. C.; Olmstead, M. M.; Lee, H. O.; Klavins, P.; Fisk, Z.; Kauzlarich, S. M.; Hermann, R. P.; Grandjean, F.; Long, G. J. *Inorg. Chem.* **2005**, *44*, 2189−2197. (f) Brown, S. R.; Kauzlarich, S. M.; Gascoin, F.; Snyder, G. J. *Chem. Mater.* **2006**, *18*, 1873−1877.
(6) (a) Chung, D.-Y.; Hogan, T.; Brazis, P.; Rocci-Lane, M.; Kannewurf, C.; Bastea, M.; Uher, C.; Kanatzidis, M. G. *Science* **2000**, *287*, 1024−1027. (b) Kim, S.-J.; Salvador, J.; Bilc, D.; Mahanti, S. D.; Kanatzidis, M. G. *J. Am Chem. Soc.* **2001**, *123*, 12704−12705. (c) Park, S. M.; Kim, S.-J.; Kanatzidis, M. G. *Inorg. Chem.* **2005**, *44*, 4979−4982.
(7) (a) Bobev, S.; Thompson, J. D.; Sarrao, J. L.; Olmstead, M. M.; Hope, H.; Kauzlarich, S. M. *Inorg. Chem.* **2004**, *43*, 5044−5052. (b) Bobev, S.; Merz, J.; Lima, A.; Fritsch, V.; Thompson, J. D.; Sarrao, J. L.; Gillessen, M.; Dronskowski, R. *Inorg. Chem.* **2006**, *45*, 4047−4054. (c) Xia, S.-Q.; Bobev, S. *Inorg. Chem.* **2006**, *45*, 7126−7132. (d) Xia, S.-Q.; Bobev, S. *Inorg. Chem.* **2007**, *46*, 874−883.

filling efficiently the available space) are deemed inadequate.[8] Examples abound, most notably among the three-dimensional networks,[9] where apparent violations of the octet rule and deviations from the optimal electron count are compensated by an interplay of the Madelung (lattice) energy and the size effects.[9−11] Consequently, these take priority over the electronic requirements, which normally are the dominating factor for the formation of the Zintl phases.[11]

As part of a broader program to better understand these aspects of the chemistry and physics of such complex intermetallics, we embarked on the study of various *d*- and *f*-element containing phases, mainly aimed at systems with one- or two-dimensional partial anionic networks. Here, we report the first series of unexpected results in relation to the synthesis and the characterization of two new ternary Zintl compounds, Yb_2CdSb_2 and Ca_2CdSb_2, the phase stability of which seems to be governed by factors that are different than the ones described above. The structures of the two title compounds are both based on corner-shared $CdSb_4$ tetrahedra forming layers with the same connectivity mode; however, regardless of the identical electronic and size requirements of the Yb^{2+} and the Ca^{2+} cations, the layers in Yb_2CdSb_2 and Ca_2CdSb_2 are packed differently. This finding is rather surprising because of the fact that virtually all other Yb and Ca counterparts are isoelectronic and isostructural.

In this sense, these unique layered structures can be viewed as rare examples of polytypes (not polymorphs), whose discovery brings a new level of understanding to the role of the cations as structure directing factors. These ideas are discussed in the context of the imaginary process of deriving these new layered structure types from some well-known structures with three-dimensional four-connected nets and are supported by electronic structure calculations, which also show strong cation preference for each arrangement.

2. Experimental Section

2.1. Synthesis. Handling of all materials was carried out inside an argon-filled glove box or under a vacuum. All elements for the syntheses were used as received: Yb (Ames Laboratory, ingot, 99.99%), Ca (Aldrich granules, 99.9%), Cd (Alfa, shot, 99.999%), Sb (Alfa, shot, 99.99%). Two different synthetic procedures were explored: on-stoichiometry reactions in welded Nb-tubes or flux-reactions in alumina crucibles. Specific temperature profiles are mentioned below; further details on the techniques and the experimental procedures are given elsewhere.[7]

2.1.1. Yb_2CdSb_2. Crystals of Yb_2CdSb_2 were initially grown from a reaction loaded with the ratio of Yb/Cd/Sb = 1:36:1. The large excess of Cd was used as a metal flux, and the experiment was intended to produce crystals of the hitherto unknown $Yb_9Cd_{4+x}Sb_9$, isostructural with the recently synthesized $Yb_9Zn_{4+x}Sb_9$.[7a] The elements were put into alumina crucibles and sealed in fused silica tubes under vacuum. The reactions were carried out using the following heating profile: (1) heating to 700 °C (below the boiling point of Cd) at a rate of 200 °C/h; (2) homogenization at this temperature for 20 h; (3) followed by a slow cooling to 400 °C at a rate of 5 °C/h. At this point the reaction mixture was taken out from the furnace and the excess of the molten Cd was removed. The reaction product consisted of needle-shaped crystals of Yb_2CdSb_2.

After the structure and the composition were established by single-crystal X-ray diffraction, several attempts to synthesize Yb_2CdSb_2 from an "on-stoichiometry" reaction in welded Nb tubes were made but proved unsuccessful. The main products of such reactions were $YbCd_2Sb_2$ ($CaAl_2Si_2$ type),[12] $Yb_{11}Sb_{10}$ ($Ho_{11}Ge_{10}$ type),[13] and $YbCd_6$ (YCd_6 type).[14,15] The Cd-flux reactions yielded the desired phase; however, the crystals were on the small side to ensure accurate resistivity measurements. Therefore, to allow for a higher reaction temperature in order to improve the size of the grown crystals, new reactions using molten lead metal, instead of cadmium, were employed. The optimized reaction conditions were as follows: a mixture of Yb, Cd, Sb, and Pb in a ratio of 2:1:2:10 was heated from room temperature to 960 °C at a rate of 200 °C/h, allowed to dwell at this temperature for 20 h, and then slowly cooled to 500 °C at a rate of 5 °C/h. The flux was subsequently removed, and the outcome of the reaction was Yb_2CdSb_2 in nearly 100% yield and excellent crystal quality.

2.1.2. Ca_2CdSb_2. Black, needle-shaped crystals of Ca_2CdSb_2 were synthesized from an analogous reaction among Ca, Cd, and Sb in molten lead, which appears to be the most accessible synthetic route to single-crystalline Ca_2CdSb_2. Numerous tries to synthesize it from stoichiometric or cadmium flux reactions failed; the major product of such reactions was $CaCd_2Sb_2$.[16] The temperature profiles employed in all of these syntheses were identical to those described above for Yb_2CdSb_2.

The crystals of both Ca_2CdSb_2 and Yb_2CdSb_2 appear dark-to-black and are very brittle. Although their surfaces slowly tarnish in air, powder X-ray diffraction confirms that the bulk materials remain unchanged after exposure to ambient air longer than 1 week.

2.2. Powder X-ray Diffraction. X-ray powder diffraction patterns were taken at room temperature on a Rigaku MiniFlex powder diffractometer, using monochromatized Cu Kα radiation. Data were collected in a $\theta-\theta$ mode ($2\theta_{max} = 80°$) with a step size of 0.04° and 10 s/step counting time. The data analysis was carried out using the JADE 6.5 software package. The position and the intensity of the peaks matched well with those calculated from the refined structures. The diffraction patterns in the low-angle region (Supporting Information, Figure S1) exhibit reflection conditions consistent with the primitive and base-centered orthorhombic symmetry of Ca_2CdSb_2 and Yb_2CdSb_2, respectively.

2.3. Single-Crystal X-ray Diffraction. Single crystals of the title compounds were selected in a glovebox and cut in Paratone N oil to suitable size for data collection: $0.06 \times 0.04 \times 0.02$ mm^3 for Yb_2CdSb_2 and $0.09 \times 0.03 \times 0.02$ mm^3 for Ca_2CdSb_2, respectively. They were then mounted on glass fibers and quickly placed under the cold nitrogen stream (ca. −153 °C) of the goniometer of a Bruker SMART CCD-based diffractometer. Intensity data covering a full sphere of the reciprocal space were collected in four batch runs at different ω and ϕ angles. The frame width was 0.4° in ω and θ, and the acquisition rate was 20 s/frame. The data collection, data integration, and cell refinement were done using the SMART and SAINT programs,[17a] respectively.

(8) (a) Mudring, A. V.; Corbett, J. D. *J. Am. Chem. Soc.* **2004**, *126*, 5277−5281. (b) Alemany, P.; Llunell, M.; Canadell, E. *Inorg. Chem.* **2006**, *45*, 7235−7241.

(9) (a) Seo, D.-K.; Corbett, J. D. *J. Am. Chem. Soc.* **2000**, *122*, 9621−9627. (b) Haussermann, U.; Amerioun, S.; Eriksson, L.; Lee, C. S.; Miller, G. J. *J. Am. Chem. Soc.* **2002**, *124*, 4371−4383. (c) Li, B.; Corbett, J. D. *Inorg. Chem.* **2006**, *45*, 3861−3863.

(10) In the most simplified terms, the three principal factors that govern the formation, the stability, and the properties of the intermetallic phases are as follows: (i) the relative sizes of the constituent atoms; (ii) the relative electronegativities of the constituent atoms; and (iii) the valence electron concentration (*vec*).

(11) (a) Seo, D.-K.; Corbett, J. D. *J. Am. Chem. Soc.* **2001**, *123*, 4512−4518. (b) Seo, D.-K.; Corbett, J. D. *J. Am. Chem. Soc.* **2002**, *124*, 415−420. (c) Li, B.; Corbett, J. D. *J. Am. Chem. Soc.* **2005**, *127*, 926−932.

(12) Artmann, A.; Mewis, A.; Roepke, M.; Michels, G. Z. *Anorg. Allg. Chem.* **1996**, *622*, 679−682.

(13) Clark, H. L.; Simpson, H. D.; Steinfink, H. *Inorg. Chem.* **1970**, *9*, 1962−1964.

(14) Xia, S.-Q.; Bobev, S. *Intermetallics* **2006**, doi:10.1016/j.intermet.2006.09.006.

(15) (a) Villars, P.; Calvert, L. D. *Pearson's Handbook of Crystallographic Data for Intermetallic Phases*, 2nd ed.; American Society for Metals: Materials Park, OH, 1991, and the desktop edition, 1997. (b) Inorganic Crystal Structure Database, Fachinformationszentrum (FIZ) Karlsruhe.

(16) Mewis, A. *Z. Naturforsch.* **1978**, *33B*, 382−384.

(17) (a) *SMART and SAINT*; Bruker AXS Inc.: Madison, Wisconsin, U.S.A., 2002. (b) Sheldrick, G. M. *SADABS*; University of Göttingen: Germany, 2003; (c) Sheldrick, G. M. *SHELXTL*; University of Göttingen: Germany, 2001.

Table 1. Selected Crystal Data and Structure Refinement Parameters for Ca_2CdSb_2 and Yb_2CdSb_2

empirical formula	Ca_2CdSb_2	Yb_2CdSb_2
formula weight	436.06 g/mol	701.98 g/mol
data collection temp	−153(2) °C	
radiation, wavelength	Mo Kα, $\lambda = 0.710\ 73$ Å	
crystal system	orthorhombic	
space group	*Pnma* (No. 62)	$Cmc2_1$ (No. 36)
unit cell dimensions	$a = 7.2536(13)$ Å	$a = 4.6184(17)$ Å
	$b = 4.6030(8)$ Å	$b = 17.418(6)$ Å
	$c = 17.521(3)$ Å	$c = 7.178(3)$ Å
unit cell volume, Z	585.0(2) Å^3, 4	577.4(4) Å^3, 4
density (ρ_{calcd})	4.951 g/cm^3	8.076 g/cm^3
absorption coefficient (μ)	14.359 mm^{-1}	44.768 mm^{-1}
goodness-of-fit	1.199	1.111
final R indices[a] [$I > 2\sigma_{(I)}$]	$R_1 = 0.0222$	$R_1 = 0.0216$
	$wR_2 = 0.0571$	$wR_2 = 0.0463$
final R indices[a] [all data]	$R_1 = 0.0237$	$R_1 = 0.0216$
	$wR_2 = 0.0578$	$wR_2 = 0.0463$

[a] $R_1 = \sum||F_o| - |F_c||/\sum|F_o|$; $wR_2 = [\sum[w(F_o^2 - F_c^2)^2]/\sum[w(F_o^2)^2]]^{1/2}$, where $w = 1/[\sigma^2F_o^2 + (0.0133 \cdot P)^2]$ for Yb_2CdSb_2 and $w = 1/[\sigma^2F_o^2 + (0.0321 \cdot P)^2 + 0.2664 \cdot P]$ for Ca_2CdSb_2, $P = (F_o^2 + 2F_c^2)/3$.

SADABS[17b] was used for semiempirical absorption correction based on equivalents ($T_{min}/T_{max} = 0.372$ and $R_{int} = 0.044$ for Yb_2CdSb_2; $T_{min}/T_{max} = 0.470$ and $R_{int} = 0.032$ for Ca_2CdSb_2). Unit cell parameters were refined using all reflections. The structures were subsequently solved by direct methods and refined by full matrix least squares on F^2 using SHELXL.[17c] For both Yb_2CdSb_2 and Ca_2CdSb_2, all five atoms in the asymmetric unit were located from the solutions and the structures were subsequently refined with anisotropic displacement parameters (Supporting Information, Figures S2 and S3 display the structures with thermal ellipsoids). Site occupations were checked for deviations from unity by freeing the site occupancy factor (SOF) of an individual atom while the remaining SOFs were kept fixed, which proved that all sites are fully occupied. Further details on the data collection and structure refinements parameters are given in Table 1; several other points worth specific mention are provided below.

2.3.1. Yb_2CdSb_2. The systematic absence of reflections with indices *hkl*, *hk*0: $h + k \neq 2n$; *h*0*l*: h or $l \neq 2n$; *h*00: $h \neq 2n$; 0*k*0, 0*kl*: $k \neq 2n$, and 00*l*: $l \neq 2n$ confirmed the base-centering of the cell and the presence of a *c*-glide along the *b*-axis. The reflection conditions were confirmed by powder X-ray diffraction as well (Figure S1). This analysis suggested three possible space groups: $Cmc2_1$ (No. 36), *Cmc*2 (No. 40), and the centrosymmetric space group *Cmcm* (No. 63). The intensity statistics were consistent with the noncentrosymmetric groups, and the structure was successfully solved in $Cmc2_1$. Attempts to solve and refine the structure in the other possible groups failed; satisfactory structure refinement of the 33 parameters against the 661 structure factors ($I_O > 2\sigma(I_O)$) was achieved only in $Cmc2_1$ (Table 1). The absolute structure coefficient (a.k.a. the Flack coefficient) was refined to be 0.09(1). The final difference Fourier map was featureless with a highest residual peak of ca. 1.5 e$^-$/Å^3 less than 1 Å away from Yb1.

2.3.2. Ca_2CdSb_2. Despite the similar unit cell parameters and the same Laue symmetry (Table 1), the reflection conditions for Ca_2CdSb_2 were very different than those of Yb_2CdSb_2. The systematic absence of reflections with indices 0*kl*: $k + l \neq 2n$; *hk*0, *h*00: $h \neq 2n$; 0*k*0: $k \neq 2n$, and 00*l*: $l \neq 2n$ established the primitive cell and the presence of *n*- and *a*-glides along the *a*- and *c*-axes, respectively, hence suggesting only two possible space groups: $Pn2_1a$ (No. 33) and *Pnma* (No. 62). The intensity statistics strongly favored a centrosymmetric model, and the structure was solved in the latter group by direct methods.[17c] Subsequent refinements confirmed an ordered structure with five unique crystallographic sites that are fully occupied. Refinements of the 31 parameters against the 639 structure factors ($I_O > 2\sigma(I_O)$) converged at low conventional residuals (Table 1) and a virtually flat difference Fourier map; the highest peak is in the order 2 e$^-$/Å^3 and it is located approximately 1.5 Å away from Cd.

Table 2. Atomic Coordinates and Equivalent Isotropic Displacement Parameters (U_{eq}[a]) for Ca_2CdSb_2 and Yb_2CdSb_2

atom	Wyckoff position	x	y	z	U_{eq} (Å^2)
		Ca_2CdSb_2 in *Pnma*			
Ca1	4*c*	0.2303(2)	1/4	0.446 84(8)	0.0133(3)
Ca2	4*c*	0.0347(2)	1/4	0.227 74(7)	0.0090(3)
Cd	4*c*	0.137 48(6)	1/4	0.650 77(3)	0.0102(1)
Sb1	4*c*	0.245 93(5)	1/4	0.816 32(2)	0.0074(1)
Sb2	4*c*	0.244 19(5)	1/4	0.071 42(3)	0.0092(2)
		Yb_2CdSb_2 in $Cmc2_1$			
Yb1	4*a*	0	0.302 47(3)	0.529 82(7)	0.0125(2)
Yb2	4*a*	0	0.478 79(3)	0.2212(1)	0.0093(2)
Cd	4*a*	0	0.098 96(5)	0.3955(2)	0.0099(2)
Sb1	4*a*	0	0.067 21(5)	0.0000(1)	0.0082(2)
Sb2	4*a*	0	0.321 52(5)	0.0109(2)	0.0098(2)

[a] U_{eq} is defined as one-third of the trace of the orthogonalized U_{ij} tensor.

Table 3. Selected Bond Distances in Ca_2CdSb_2 and Yb_2CdSb_2

atom pair	distance (Å)	atom pair	distance (Å)
Ca_2CdSb_2		Yb_2CdSb_2	
Cd − Sb2 × 2	2.8226(5)	Cd − Sb2 × 2	2.817(1)
Sb1	2.8981(8)	Sb1	2.892(2)
Sb1	3.0054(8)	Sb1	2.990(2)
Sb1 − Cd	2.8981(8)	Sb1 − Cd	2.892(2)
Cd	3.0054(8)	Cd	2.990(2)
Sb2 − Cd × 2	2.8226(5)	Sb2 − Cd × 2	2.817(1)
Ca1 − Sb2 × 2	3.177(1)	Yb1 − Sb2 × 2	3.165(1)
Sb1 × 2	3.249(1)	Sb1 × 2	3.245(1)
Sb2	3.541(2)	Sb2	3.469(2)
Sb2	3.741(2)	Sb2	3.739(2)
Ca2 − Sb2	3.132(1)	Yb2 − Sb2	3.128(1)
Sb1 × 2	3.168(1)	Sb1 × 2	3.159(1)
Sb1 × 2	3.200(1)	Sb1 × 2	3.198(1)
Cd × 2	3.375(1)	Cd × 2	3.358(1)
Cd × 2	3.573(1)	Cd × 2	3.554(1)

In the last refinement cycles, the atomic positions were standardized using STRUCTURE TIDY.[18] Final positional and equivalent isotropic displacement parameters and important bond distances and angles are listed in Tables 2 and 3, respectively. Further information in the form of CIF has been deposited with FIZ Karlsruhe, 76344 Eggenstein-Leopoldshafen, Germany (e-mail: crysdata@fiz. karlsruhe.de), depository number CSD 391389 for Yb_2CdSb_2 and CSD 391390 for Ca_2CdSb_2.

2.4. Property Measurements. Detailed descriptions of the magnetic susceptibility and the electrical resistivity measurements are provided as Supporting Information. The data show essentially temperature-independent paramagnetism for Yb_2CdSb_2. The latter is also a poor metal ($\rho_{295} = 2.25$ mΩ · cm; $\rho_{10} = 1.2$ mΩ · cm), whereas Ca_2CdSb_2 is a semiconductor with an estimated band gap of about 0.19(5) eV. Graphical representations of $\chi(T)$ and $\chi^{-1}(T)$ are shown in Figure S4; the resistivity data are plotted in Figure S5, respectively.

2.5. Electronic Structure Calculations. Electronic structure calculations were performed using the linear muffin-tin orbital (LMTO) method[19] with the aid of the TB-LMTO program.[20] Exchange and correlation were treated in the local density approximation (LDA).[21] All relativistic effects except for spin−orbit coupling were taken into

(18) (a) Parthe, E.; Gelato, L. M. *Acta Crystallogr.* **1984**, *A40*, 169−183. (b) Gelato, L. M.; Parthe, E. *J. Appl. Crystallogr.* **1987**, *20*, 139−143.
(19) (a) Andersen, O. K. *Phys. Rev. B* **1975**, *12*, 3060−3083. (b) Andersen, O. K.; Jepsen, O. *Phys. Rev. Lett.* **1984**, *53*, 2571−2574. (c) Andersen, O. K.; Jepsen O.; Glötzel, D. In *Highlights of Condensed Matter Theory*; Bassani, F., Fumi, F., Tosi, M. P., Eds.; North Holland: New York, 1985. (d) Andersen, O. K. *Phys. Rev. B* **1986**, *34*, 2439−2449. (e) Skriver, H. L. *The LMTO Method*; Springer: Berlin, 1984.
(20) Jepsen, O.; Andersen, O. K. *The Stuttgart TB-LMTO Program, Version 4.7*.
(21) Von Barth, U.; Hedin, L. *J. Phys. C* **1972**, *5*, 1629−1642.

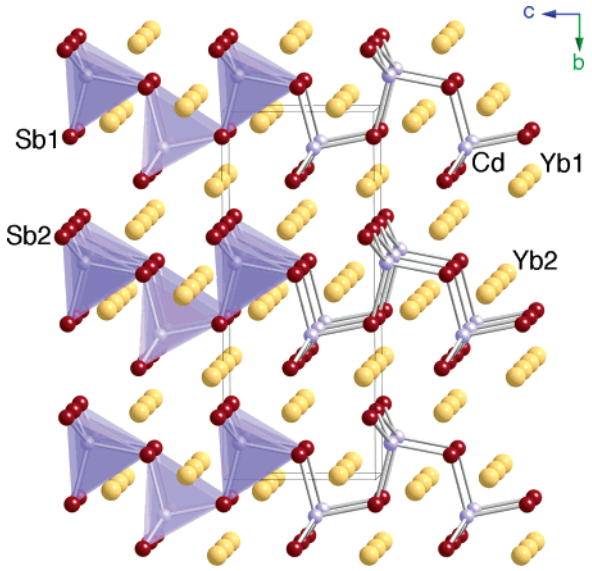

Figure 1. Structure of Yb_2CdSb_2 ($Cmc2_1$), viewed down the *a*-axis. The Sb atoms are drawn as deep red spheres, and the Cd atoms are shown as light-indigo spheres, which center the translucent tetrahedra, respectively. The Yb atoms are drawn as yellow spheres, and the unit cell is outlined.

account by the scalar relativistic approximation.[22] The basis set included the 4*s*, 4*p*, 3*d* orbitals for Ca; 5*s*, 5*p*, 4*d*, 4*f* orbitals for Cd and Sb; and the 6*s*, 6*p*, 5*d*, 4*f* orbitals for Yb. The Ca 4*p*, Yb 6*p*, Cd 4*f*, and Sb 4*d*, 4*f* orbitals were treated with the downfolding technique.[23] In both cases, the *k*-space integrations were performed by the tetrahedron method[24] using a total of 600 irreducible *k*-points in the Brillouin zone. The Fermi level was selected as the energy reference ($\epsilon_F = 0$ eV).

3. Results and Discussion

3.1. Structure Description. Yb_2CdSb_2 and Ca_2CdSb_2 are new layered compounds, the structures of which contain identical building units, Cd-centered tetrahedra of Sb that share corners to form two-dimensional polyanionic sheets $^2_\infty[CdSb_2]^{4-}$, separated by Yb^{2+} and Ca^{2+} cations, respectively. Despite this and despite the comparable unit cell parameters and chemical formulas, the title compounds are not isostructural (Table 1). The major difference is in the way the layers are arranged in space; hence, the two structures can be considered as polytypes, i.e., as built up of layers of identical topology and composition but with different stacking sequences. These two "polytypes" are not easily related by the crystallographic *translationgleiche* (*t*) or *klassengleiche* (*k*) group−subgroup relations; however, the structures of both Yb_2CdSb_2 and Ca_2CdSb_2 can formally be derived from the hypothetical compounds YbCdSb and CaCdSb, respectively, both with the ubiquitous TiNiSi type.[15] These considerations are discussed in detail in the following paragraphs.

3.1.1. Yb_2CdSb_2. Yb_2CdSb_2 crystallizes in a new type (Pearson's symbol *oC*20) with the orthorhombic space group $Cmc2_1$ (Figure 1), and its structure contains two antimony, one cadmium, and two ytterbium atoms in the asymmetric unit, all in special positions with $x = 0$ (Tables 1 and 2). The structure is best described as made up of infinite layers of $CdSb_4$ tetrahedra, which are joined together through corners along the

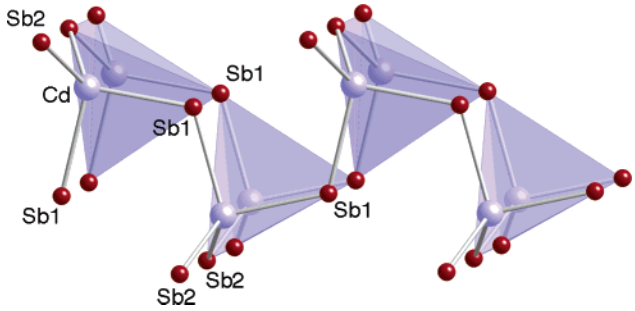

Figure 2. A close-up view of a section of the $^2_\infty[CdSb_2]^{4-}$ layer in Yb_2CdSb_2, projected approximately along the *a*-axis. Relevant bond distances and angles are listed in Table 3.

a- and *c*-axes as shown in Figure 2. The layers are stacked along the direction of the longest crystallographic axis, the *b*-axis. Due to the lack of inversion symmetry and the centering of the unit cell, all layers have "identical geometry" but are not positioned exactly on top of each other. In that sense, the stacking sequence of the $^2_\infty[CdSb_2]^{4-}$ slabs can be denoted as AAAA, keeping in mind that adjacent layers are displaced by a translation halfway along the *a*-axis (the viewing direction in Figure 1). Layers of Yb^{2+} cations that counterbalance the charges fill the space between the anionic layers.

The $CdSb_4$ tetrahedra are distorted (Figure 2), as evidenced from the Cd−Sb bond distances and from the Sb−Cd−Sb angles, which range from 2.817(1) to 2.990(2) Å and from 93.50(3)° to 113.71(3)°, respectively (Table 3). These values compare well with those reported for other ternary A−Cd−Sb phases (A = alkali, alkaline-earth or rare earth metal) the structures of which are also based on $CdSb_4$ tetrahedra; for example, the Cd−Sb contacts in the layered structure of $YbCd_2Sb_2$ ($P\bar{3}m1$, $CaAl_2Si_2$ type) range from 2.864 to 2.970 Å, while the corresponding angles vary from 88.55° to 110.43°.[12] Another useful comparison can be made with the compound NaCdSb (*Pnma*, TiNiSi type), the three-dimensional structure of which is based on corner- and edge-shared $CdSb_4$ tetrahedra (Figure S6).[25] The latter are similarly distorted: Cd−Sb distances range from 2.864 to 2.977 Å, while the corresponding angles vary from 104.29° to 115.63°.[25] Similar bond distances and angles are reported in the channel-like structure of $Sr_{11}Cd_6Sb_{12}$ as well.[26] There are no Cd−Cd or Sb−Sb distances that signify bonding interactions; the shortest Sb−Sb contacts are between pairs of Sb1 atoms within the layers, $d_{Sb1-Sb1} = 4.285(2)$ Å. The shortest interlayer distances, 4.430(2) Å, are between Sb1 and Sb2 in the direction parallel to the *b*-axis.

The coordination polyhedra of the Yb atoms deserve special mention too. There are two crystallographically independent Yb sites, both having the same point symmetry, but their local environments are very different (Figure 3). The coordination of Yb1 resembles that of a distorted octahedron, where the Yb cation is tightly coordinated by four Sb atoms in "equatorial" position, bond distances 3.165(1) and 3.245(1) Å, respectively (Table 3). These four antimony atoms lie in a plane, with the Yb cation positioned 0.174 Å away from it in a direction toward the next nearest Sb ($d_{Yb1-Sb2} = 3.469(2)$ Å). The sixth Sb atom caps the open square face from the opposite side, and it is located 3.739(2) Å away from Yb1 (Figure 3 left). Both "axial"

(22) Koelling, D. D.; Harmon, B. N. *J. Phys. C* **1977**, *10*, 3107−3114.
(23) Lambrecht, W. R. L.; Andersen, O. K. *Phys. Rev. B* **1986**, *34*, 2439−2449.
(24) Blöchl, P. E.; Jepsen, O.; Andersen, O. K. *Phys. Rev. B.* **1994**, *49*, 16223−16233.
(25) Savelsberg, G.; Schäfer, H. *Z. Naturforsch.* **1978**, *33B*, 370−373.
(26) Park, S.-M.; Kim, S.-J. *J. Solid State Chem.* **2004**, *177*, 3418−3422.

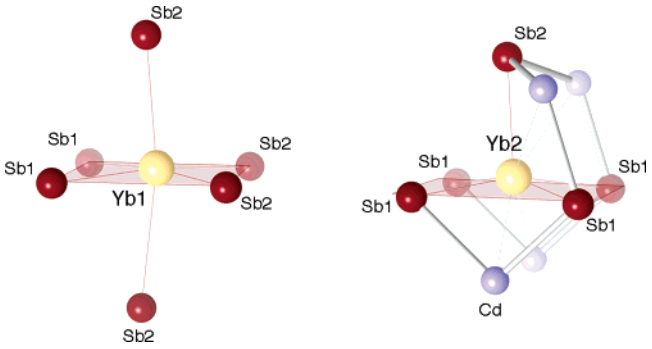

Figure 3. Detailed view of the Yb coordination in the structure of Yb_2CdSb_2. Color code the same as that in Figure 1. Relevant bond distances are given in Table 3. The coordination polyhedra of Ca in Ca_2CdSb_2 are identical.

antimony atoms are almost equidistantly positioned with respect to the four "equatorial" Sb atoms. The closest Cd atoms to Yb1 are 3.674(2) and 3.895(1) Å away. Such distances are 7 to 14% greater than the corresponding sums of the Pauling's metallic radii of Yb and Cd (CN 12)[27] and, therefore, are not considered as part of the first coordination sphere.

The second ytterbium cation (Yb2) is coordinated by five antimony atoms with Yb−Sb distances falling in the narrow range from 3.128(1) to 3.198(1) Å (Table 3). The shape of the Yb2 coordination polyhedron most closely resembles a square pyramid, which is a rare occurrence in the crystal chemistry of ytterbium. Four of the five antimony atoms form a rectangle, and the Yb cation sits 0.422 Å above it in a direction toward the fifth antimony, Sb2 (Figure 3 right). Interestingly, there is another antimony, Sb2, that can cap the equatorial "square" face from the opposite side; yet, at a distance of 4.052(2) Å, such contact (much longer that the sum of the corresponding radii and not shown in Figure 3) arguably represents any significant interaction. Yb2 also neighbors four Cd atoms at distances from 3.358(1) to 3.554(1) Å, and they cap adjacent edges of the antimony square pyramid and bring the total coordination number to CN 9.

The noticeably different coordination of Yb2 could mean disparity in the electronic state of the two nonequivalent cations; we note that Yb can exist as both Yb^{2+} (f^{14}) and Yb^{3+} (f^{13}) and there are many documented examples of Yb intermetallics, where divalent and trivalent Yb occupy sites with different coordination.[28,29] In spite of this, the fact that the very same characteristics are observed in the structure of the Ca counterpart suggests that this is not the case in Yb_2CdSb_2. These results are corroborated by the magnetic susceptibility data (Figure S4).

3.1.2. Ca_2CdSb_2. Ca_2CdSb_2 crystallizes in the orthorhombic space group *Pnma* (Table 1), and its structure contains two antimony, one cadmium, and two calcium atoms in the asymmetric unit, all in special positions with $y = 1/4$ (Table 2). We point out again that although the unit cell parameters are very similar to those of Yb_2CdSb_2 and despite the fact that many Yb intermetallics have their Ca counterparts, Yb_2CdSb_2 and Ca_2CdSb_2 are closely related but are *not* isostructural. The structure of Ca_2CdSb_2 (Figure 4), just like that of Yb_2CdSb_2, is built up of infinite $^2_\infty[CdSb_2]^{4-}$ layers stacked along the direction of the

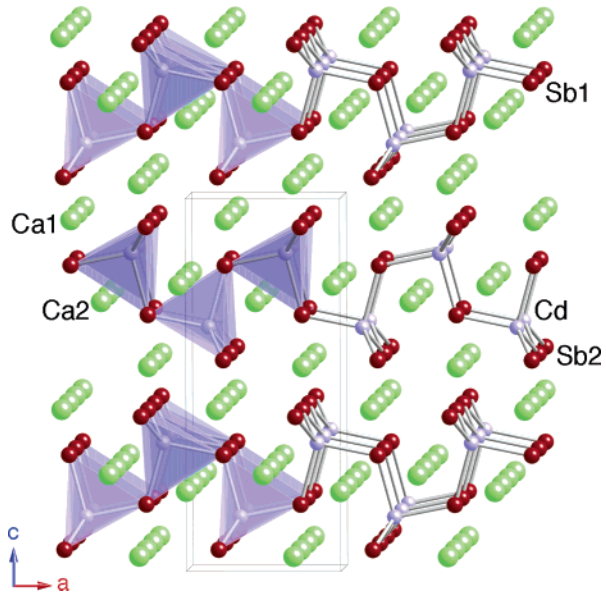

Figure 4. Structure of Ca_2CdSb_2 (*Pnma*), viewed down the *b*-axis. The Cd and Sb atoms are shown with the same colors as those in Yb_2CdSb_2 (Figure 1). The Ca atoms are shown as green spheres, and the unit cell is outlined.

longest crystallographic axis, the *c*-axis in this instance, with Ca^{2+} cations filling the space between them. The layers are again based on $CdSb_4$ tetrahedra, which are joined together through corners along the *a*- and *b*-axes (Figure 4). The Cd-centered tetrahedra are similarly distorted as evidenced from the Cd−Sb bond distances and from the Sb−Cd−Sb angles, varying from 2.8226(5) to 3.0054(8) Å and from 93.69(2)° to 113.33(1)°, respectively (Table 3).

The topology of layers in Ca_2CdSb_2, of course, is identical to the one described above for the example of Yb_2CdSb_2; the major difference here is in the way they are stacked. Because of the inversion symmetry, the stacking of the $^2_\infty[CdSb_2]^{4-}$ slabs is in alternating sequence and can be denoted as $AA^{-1}AA^{-1}$ (A^{-1} stands for the inversion image of A). In that sense, Yb_2CdSb_2 and Ca_2CdSb_2 are best described as polytypes, the structures of which feature building blocks with identical topology, but which are stacked in different manners. This situation is reminiscent with the rare-earth silicides and germanides crystallizing with the orthorhombic Sm_5Ge_4 and Gd_5Si_4 types, where subtle changes in the crystal structures are related to sets of intralayer Si−Si or Ge−Ge bonds.[30] Such compounds, particularly in the Gd_5Si_4−Gd_5Ge_4 system, have recently received increased attention, and systematic studies of the magnetic and crystallographic transformations in these phases suggest that their diverse and unique properties originate from the reversible breaking of specific intralayer bonds in the crystal structure.[30] The comparison could be extended toward many antimony and bismuth chalcogenides, the structures of which form series of closely related homologues.[31]

Independent of the difference in the packing of the polyanionic layers, the coordination of the cations remains the same in both Yb_2CdSb_2 and Ca_2CdSb_2. There are two crystallographi-

(27) Pauling, L. *The Nature of the Chemical Bond*, 3rd ed.; Cornell University Press: Ithaca, NY, 1960; p 402.
(28) Ahn, K.; Tsokol, A. O.; Mozharivskyj, Y.; Gschneidner, K. A.; Pecharsky, V. K. *Phys. Rev. B* **2005**, *72*, 054404.
(29) Tobash, P. H.; Bobev, S. *J. Am. Chem. Soc.* **2006**, *128*, 3532−3533.
(30) (a) Mozharivskyj, Y.; Pecharsky, A. O.; Pecharsky, V. K.; Miller, G. J. *J. Am. Chem. Soc.* **2005**, *127*, 317−324. (b) Meyers, J.; Chumbley, S.; Choe, W.; Miller, G. J. *Phys. Rev. B* **2002**, *66*, 012106.
(31) Poudeu, P. F. P.; Kanatzidis, M. G. *Chem. Commun.* **2005**, *21*, 2672−2674.

cally independent Ca sites, again both with the same point symmetry but with different local environments (Figure 3). Ca1 sits at the center of a very distorted octahedron, where it interacts with two Sb1 and two Sb2 atoms in an "equatorial" position, bond distances 3.249(1) and 3.177(1) Å, respectively (Table 3). The Ca cation is 0.179 Å away from the plane of those four antimony atoms. The other two Sb atoms cap the open square face from both sides and are much further away from Ca1, 3.541(2) and 3.741(2) Å (Figure 3 left). Ca2, similar to the case for Yb2, is more tightly coordinated by five antimony atoms arranged in space as a square pyramid. The Ca−Sb distances fall in the narrow range from 3.132(1) to 3.200(1) Å (Table 3) and compare very well with those observed in Yb_2CdSb_2. Ca2 also has four Cd neighbors at distances 3.375(1) and 3.573(1) Å, respectively.

3.2. Structural Relationships and Electron Count. Perhaps the most interesting feature of these structures is in the way they are related to the structure of the hypothetical compounds YbCdSb and CaCdSb (TiNiSi type, Pearson's symbol *oP*12, space group *Pnma*).[15] Many intermetallic phases are known to crystallize with this ubiquitous type (including the archetype $CeCu_2$),[15] and thorough structure descriptions can be found in several earlier publications.[32] For the sake of clarity, here we point out only that the structures of YbCdSb and CaCdSb (reformulated for convenience as $A_2Cd_2Sb_2$, A = Ca, Yb or perhaps another divalent metal) can be viewed as three-dimensional four-connected nets $^3_\infty[Cd_2Sb_2]^{4-}$ and A^{2+} cations filling the empty space within the polyanionic framework. Semiempirical band structure calculations, coupled with precise structure determinations on a series of isostructural compounds, show that the network bonding becomes increasingly stronger as the valence electron count is increased from 20 electrons in CaPdIn to 28 electrons in CaPdSb.[32] However, the calculations for systems with more than 32 electrons show that the stability of the framework sharply decreases.[33] Therefore, it is not surprising that the isostructual and isoelectronic CaAgSb, YbAgSb, and NaCdSb having 32 electrons per unit cell are found to be the most electron-rich phases with this structure.[32] The in-depth analyses of the crystal overlap populations for the three different types of bonds involving the tetrahedrally coordinated *d*-metal clearly indicate that as the valence electron concentration increases, antibonding states of predominantly one kind are being populated. Interestingly, these turn out to be originating from the shortest Cd−Sb bonds, i.e., those interactions that "fuse" the tetrahedral units through common edges to form a 3D-network (Supporting Information, Figure S6).

Following these arguments, it is evident that the $A_2Cd_2Sb_2$ compounds in question, having 36 electrons, will not be stable with the same three-dimensional structure. In fact, no equiatomic compounds of the alkaline-earth metals, group 12 transition metal, and the pnicogens have been discovered so far.[15] The excess valence electrons, obviously, cannot be tolerated in such three-dimensional four-connected nets, and it will require some sort of structural rearrangement so that the effect of the antibonding states is diminished. One such means will involve the formal removal of one-half of the Cd atoms, thereby

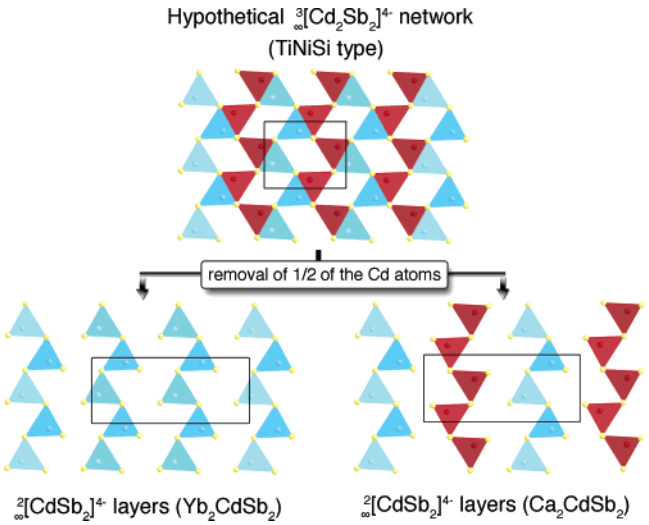

Figure 5. A schematic representation of the way the structures of Yb_2CdSb_2 and Ca_2CdSb_2 are related to those of the hypothetical compounds YbCdSb and CaCdSb. The formal derivation of the $^2_\infty[CdSb_2]^{4-}$ layers through the "patterned" removal of one-half of the Cd atoms in the three-dimensional four-connected network with the ubiquitous TiNiSi type is emphasized (see text for details).

reducing the dimensionality of the polyanionic subnetwork as schematically shown in Figure 5. This imaginary process affords the derivation of the layered structure of Yb_2CdSb_2 by breaking the "red" tetrahedra in a consecutive manner and moving one of the Yb sites in a direction toward the created vacancy to compensate for the "empty space". Similarly, the structure of Ca_2CdSb_2 can be derived by the alternating elimination of "red" and "blue" tetrahedra (inversion images), respectively, and the appropriate resizing of the unit cell (note that the different colors emphasize the center of symmetry in the parent structure in Ca_2CdSb_2 and the lack of inversion symmetry in Yb_2CdSb_2). Using the same scheme, it is conceivable that the removal of more Cd, 2/3, for example, will result in the formation of infinite chains of corner-shared $[CdSb_4]$ tetrahedra and the formulas of such hypothetical compounds will be Ca_3CdSb_3 and Yb_3CdSb_3. Although no such compounds are known so far, there are related compounds, whose structures feature such one-dimensional chains, such as Ca_3AlAs_3 and Eu_3InP_3 to name just a few.[34,5e]

A completely different mechanism for reducing the valence electron concentration and thereby the dimensionality of the polyanionic framework will be through the exclusion of a cation and the subsequent reconstruction of the layers. This will lead to the realization of $YbCd_2Sb_2$ and $CaCd_2Sb_2$ with the layered $CaAl_2Si_2$ type.[15] Elaborate description of this structure type can be found elsewhere;[7b,35] since such a transformation is beyond the scope of the present discussion, only a schematic representation of this imaginary process is provided as a reference in the Supporting Information (Figure S7).

These considerations prompt the attention to another interesting observation regarding the formal electron count in the series of compounds discussed above. For example, using the Zintl rules,[1−3] the structures of Yb_2CdSb_2 and Ca_2CdSb_2 can be

(32) Nuspl, G.; Polborn, K.; Evers, J.; Landrum, G. A.; Hoffmann, R. *Inorg. Chem.* **1996**, *35*, 6922−6932 and the references therein.
(33) The electron count does not include the *d*-electrons; only *s*- and *p*-electrons are considered. The number is per unit cell (*Z* = 4), following the electron counting scheme from ref 32.
(34) Cordier, G.; Schäfer, H. *Angew. Chem., Int. Ed. Engl.* **1981**, *20*, 466−466.
(35) (a) Zheng, C.; Hoffmann, R.; Nesper, R.; von Schnering, H. G. *J. Am. Chem. Soc.* **1986**, *108*, 1876. (b) Zheng, C.; Hoffmann, R. J. *Solid State Chem.* **1988**, *72*, 58. (c) Burdett, J. K.; Miller, G. J. *Chem. Mater.* **1990**, *2*, 12.

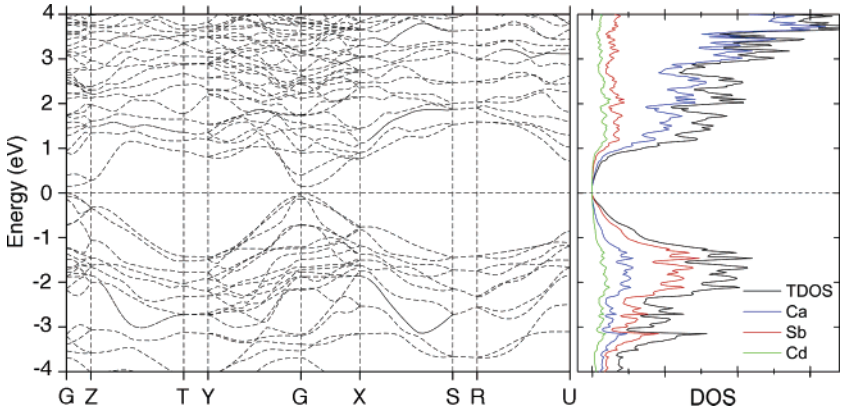

Figure 6. Calculated band structure for Ca_2CdSb_2 (left). Drawn on the same energy scale is the projected total and partial DOS (right). Contributions from different atoms are color-coded.

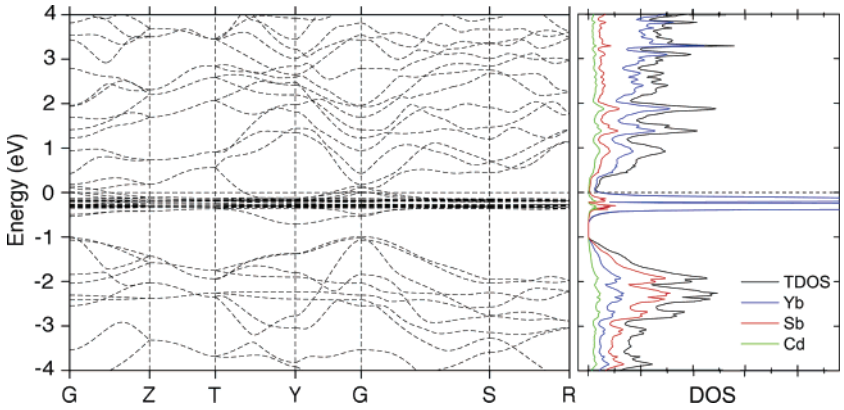

Figure 7. Calculated band structure for Yb_2CdSb_2 (left). Drawn on the same energy scale is the projected total and partial DOS (right). Contributions from different atoms are color-coded.

Table 4. Integrated −COHP (eV) for the Average Cation−Antimony and Cadmium−Antimony Interactions in Ca_2CdSb_2 and in Yb_2CdSb_2[a]

	Ca_2CdSb_2		Yb_2CdSb_2	
	Pnma	***Cmc2₁***	***Pnma***	***Cmc2₁***
Ca1(Yb1)-Sb	0.580	0.510	0.178	0.401
Ca2(Yb2)-Sb	0.736	0.732	0.412	0.617
Cd-Sb	1.555	1.538	1.669	1.459
d orbital population [Ca1 or Yb1]	0.642	0.605	0.736	0.644

[a] The calculations are performed on the real structures and on the hypothetical counterparts by using the structural parameters from Tables 1 and 2. Values for the less stable model in each case are highlighted in blue.

rationalized as $[Yb^{2+}]_2[Cd^{2+}][Sb^{3-}]_2$ and $[Ca^{2+}]_2[Cd^{2+}][Sb^{3-}]_2$, respectively, i.e., as typical charge-balanced Zintl phases. Such a conclusion, although based on an overly simplistic concept, is nicely supported by the band structure calculations and by the magnetic susceptibility measurements. Following the same formalism, it is evident that charge neutrality can be achieved only for the "2−1−2" (or "1−2−2") stoichiometry. CaCdSb and Ca_3CdSb_3 for example will be one-electron rich and one-electron deficient (per formula), respectively. On the contrary, the triel analogues (Tr = Al, Ga, In) of the above-mentioned "3−1−3" compounds, in which the tetrahedrally coordinated Cd^{2+} are substituted by Tr^{3+} (e.g., Eu_3InP_3[5e]) or the alkali-metal counterpart of the electron-rich CaCdSb (e.g., NaCdSb[25]), will be charge-balanced Zintl phases too. Another way to provide the optimal valence electron concentration will be by using small cations, such as Li, Be, or Mg, which can occupy small tetrahedral voids in the structure (created by the removal of one-half of the Cd atoms, Figure S8). This last point deserves a special mention here because it could be used as a practical guide for the prediction of new compounds capable of existence within these families and beyond. To further illustrate that idea, we point out the recently reported compounds $A_2LiInGe_2$ (A = Ca, Sr), which have a layered structure made up of $^2_\infty[InGe_2]^{5-}$ layers.[36] The geometry of these layers and the coordination of the A-cations in this structure (Pearson's symbol *oP*24, space group *Pnma*) are virtually the same as those for the building

(36) Mao, J.-G.; Xu, Z. -H.; Guloy, A. M. *Inorg. Chem.* **2001**, *40*, 4472−4477.

blocks in the structure of Ca_2CdSb_2 (Pearson's symbol *oP*20, space group *Pnma*). The difference lies in the presence of the extra cation, Li, without which the structure will be electron deficient and probably unstable, $[Ca^{2+}]_2[Li^+][In^{3+}][Ge^{4-}]_2$.[36] Importantly, the small lithium cations do not cause additional distortions of the layers and occupy tetrahedral voids as predicted above.

3.3. Electronic Structure and Properties. Self-consistent electronic band structure calculations were performed on both compounds, and the results are shown in Figure 6 for Ca_2CdSb_2 and in Figure 7 for Yb_2CdSb_2, respectively. The calculated electronic structures are consistent with the formal electron count as discussed above and with the physical properties; Ca_2CdSb_2 is a direct band gap semiconductor ($E_g \approx 0.16$ eV), in which the electrons in the valence band could be activated to the conduction band through the high symmetry *k*-point G (0,0,0). However, for Yb_2CdSb_2 the gap closes and there are some small overlaps between the valence and the conduction bands, again at the G-point. These computational results are fully corroborated by the experimentally measured resistivities of both Ca_2CdSb_2 and Yb_2CdSb_2 (Figure S5). Such differences in the resistivity of nominally isoelectronic phases are not unusual as seen in the example of the recently reported $CaZn_2Sb_2$ and $YbZn_2Sb_2$, where the existence of a solid solution of $Ca_{1-x}Yb_xZn_2Sb_2$ provides for a unique way of varying the electronic properties.[37]

Plotted on the same energy scale in Figure 6 are the total and the partial density-of-states (DOS) diagrams for Ca_2CdSb_2. From the plots, it is clear that the bands around the Fermi level are predominantly contributed by Ca and Sb states. Detailed analysis of the DOS reveals that these are mainly composed of Ca-3*d* and Sb-5*p* orbitals, suggesting that this *p*−*d* mixing should have a strong effect on the electronic properties of this compound. We note that the mixing between the cation's *d*-bands and the *p*-bands of the anion has been the subject of several recent publications.[8,38] The specifics have been analyzed in detail and shown to play an important role and account for the metallicity of some classical Zintl phases.[8,38] In Ca_2CdSb_2, as mentioned already, the nearest valence bands and conduction bands around the Fermi level are separated in energy, which makes the Fermi level fall into a gap in the total DOS. Thus, the valence electrons are basically localized in the Ca−Sb and Cd−Sb sublattices, both of which are electron precise.

The corresponding total and partial DOS (Figure 7) curves for Yb_2CdSb_2 are very similar to those of Ca_2CdSb_2, and the states around the Fermi level are predominantly contributed by Yb- and Sb-bands. These are mostly originating from Yb-5*d* and Sb-5*p* orbitals, which indicate that *p*−*d* mixing between cationic and anionic states again plays an important role on the electronic structure. However, because of the filled 4*f* orbitals, the Fermi level is now shifted to just above the Yb-4*f* states and the band gap disappears. This characteristic, as well as the small mixing between Yb-4*f* and -5*d* orbitals near the Fermi level, explains the poor metallic behavior for Yb_2CdSb_2. Such an admixture of *f*- and *d*-states is very common in rare-earth-based intermetallics[39] and usually accounts for the long-distance magnetic interaction when direct overlap could not be reached (RKKY mechanism).[40]

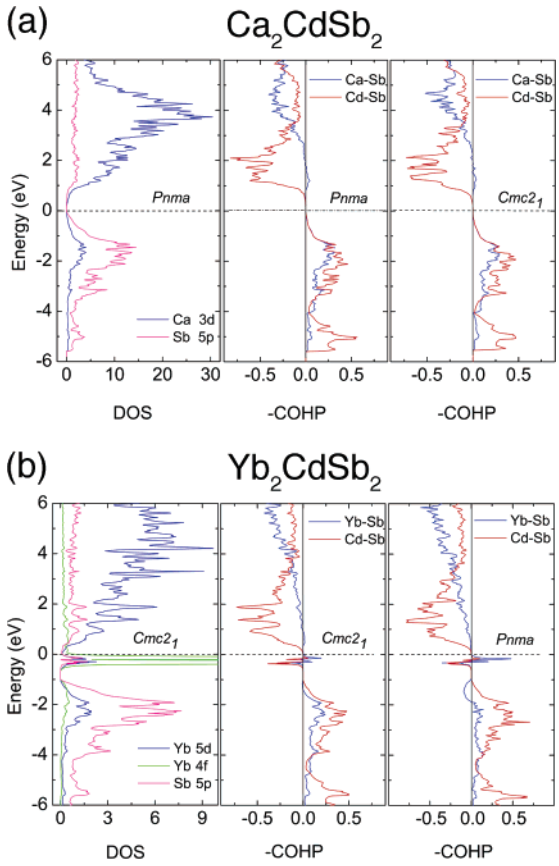

Figure 8. Projected partial DOS and integrated −COHP diagrams for selected cation−anion and anion−anion interactions for Ca_2CdSb_2 (a) and Yb_2CdSb_2 (b). Calculations are performed on the "real" structures (*Pnma* for Ca_2CdSb_2; *Cmc*2$_1$ for Yb_2CdSb_2) and on the hypothetical structures by swapping the cations. See text for details.

The interpretation of the DOS, combined with the crystal orbital Hamilton populations (COHP) presented in Figure 8, leads to the conclusion that both Ca_2CdSb_2 and Yb_2CdSb_2 have the same electronic requirements (32 valence electrons per unit cell) and that both are electron precise phases. These computational results are fully corroborated by the temperature-dependent magnetic susceptibility data (showing divalent oxidation state for the Yb, Figure S4) and by the resistivity measurements (Figure S5), which suggest narrow-gap semiconducting behavior for Ca_2CdSb_2 and poor-metallic behavior for Yb_2CdSb_2. However, it must be pointed out that the small intra-atomic mixing between the Yb-4*f* and -5*d* orbitals causes weakening of the interactions as evidenced by the Yb−Sb COHP (Figure 8); the bands with a clear mixing have a nonbonding or even slightly antibonding character.

From all of the above, the physical properties of the title compounds can be explained and understood. However, the question why the cations and the anions in these two compounds pack differently has not been answered yet; after all the

(37) Gascoin, F.; Ottensmann, S.; Stark, D.; Haile, S. M.; Snyder, G. J. *Adv. Funct. Mater.* **2005**, *15*, 1860−1864.
(38) (a) Li, B.; Mudring, A.-V.; Corbett, J. D. *Inorg. Chem.* **2003**, *42*, 6940−6945. (b) Mudring, A.-V.; Corbett, J. D. *Inorg. Chem.* **2005**, *44*, 5636−5640.
(39) (a) Dronskowski, R. *Computational Chemistry of Solid State Materials: A Guide for Materials Scientists, Chemists, Physicists and others*; Wiley-VCH: Weinheim, Germany, 2005. (b) Bobev, S.; Bauer, E. D.; Thompson, J. D.; Sarrao, J. L.; Miller, G. J.; Eck, B.; Dronskowski, R. J. *Solid State Chem.* **2004**, *177*, 3545.
(40) Kittel, C. *Solid State Physics*; Academic Press: New York, 1968.

$^2_\infty[CdSb_2]^{4-}$ layers are identical and the Yb^{2+} or Ca^{2+} have very close cationic sizes and similar coordination requirements.[27] Therefore, further calculations were carried out by interchanging the structures (Figure 8). The COHPs for several atomic interactions were compared and contrasted, and the results indeed indicate a strong cation preference for each arrangement (Table 4). In particular, robust indicators are the interlayer Yb1−Sb interactions in Yb_2CdSb_2, which become much weaker upon changing the symmetry from $Cmc2_1$ to *Pnma* (Table 4); recall that cations' *d*-orbitals and Sb-5*p* orbitals mix and contribute significantly for the DOS near the Fermi level. In that sense, the optimization of the interlayer Ca1−Sb and Yb1−Sb interactions would have an important role in the structure selection; in Ca_2CdSb_2, for example, the centrosymmetric lattice provides a slightly better overlap between the Ca-3*d* and Sb-5*p* orbitals than the noncentrosymmetric one (Table 4). On the contrary, for Yb_2CdSb_2, the centrosymmetric lattice provides poorer overlap between the cation and anion states. Evidently, with more electrons filled into the *d* orbitals of Ca1, the interlayer interactions can be strengthened, whereas this will have an inverse effect if the cations were ytterbiums. Thus, Yb_2CdSb_2 is expected to be more stable if it crystallizes with the noncentrosymmetric C-centered structure.

4. Conclusions

Two new ternary compounds, Ca_2CdSb_2 and Yb_2CdSb_2, have been synthesized and structurally characterized. Despite the similarity in their chemical formulas and unit cell parameters, the structures of the title compounds are unexpectedly different. Both feature unique layered structures that contain very similar building units, which are based on Cd-centered tetrahedra of Sb to form layers, $^2_\infty[CdSb_2]^{4-}$. Such two-dimensional structures of corner-shared tetrahedral units are very rare among the transition-metal phases but are well-known in main-group chemistry[2] and, in particular, for some classes of silicates and alumino-silicates.

Another remarkable aspect of the crystal chemistry of Ca_2CdSb_2 and Yb_2CdSb_2 is that, in both structures, the polyanionic layers have identical topology and composition but are stacked in different manners. Therefore, the two structures can be considered as unusual examples of intermetallic polytypes, which is a surprising finding since the ionic radii of the Yb^{2+} and the Ca^{2+} countercations are nearly identical, and both compounds are expected to be isostructural. Furthermore, the layered structures of Ca_2CdSb_2 and Yb_2CdSb_2 are closely related to the TiNiSi-type structure with a three-dimensional four-connected network on one hand and the Ca_3AlAs_3 type with one-dimensional chains on the other. The imaginary process of reducing the dimensionality involves the formal removal of tetrahedrally coordinated Cd atoms in order to keep optimal valence electron concentration. In this sense, our combined experimental and theoretical study of the bonding in these new phases brings new understanding of the role of the cations as structure directing factors.

Acknowledgment. Svilen Bobev acknowledges financial support from the University of Delaware Research Foundation (UDRF) and from the University of Delaware through a start-up grant. We also thank Prof. Edmund R. Nowak and Arif Ozbay (Department of Physics and Astronomy, University of Delaware) for their assistance with the resistivity measurements.

Supporting Information Available: X-ray crystallographic files in CIF format (for Yb_2CdSb_2 and for Ca_2CdSb_2), along with graphical representations of the experimental and simulated powder patterns, plots of the crystal structures with anisotropic displacement parameters, plots of the magnetic susceptibility measurements for Yb_2CdSb_2, and a schematic representation of the way the structures of $YbCd_2Sb_2$ and $CaCd_2Sb_2$ are related to those of the hypothetical compounds YbCdSb and CaCdSb. This material is available free of charge via the Internet at http://pubs.acs.org.

JA069261K